CONF-950857--4

UCRL-JC-120325
PREPRINT

Series Hybrid Vehicles and Optimized Hydrogen Engine Design

J. Ray Smith, Salvador Aceves,
and Peter Van Blarigan

This paper was prepared for submittal to the
1995 SAE Future Transportation Technology Conference & Exposition
Costa Mesa, CA
August 7–10, 1995

May 10, 1995

Lawrence Livermore National Laboratory

DISCLAIMER

SERIES HYBRID VEHICLES AND OPTIMIZED HYDROGEN ENGINE DESIGN

J. Ray Smith, Salvador Aceves and Peter Van Blarigan*
Lawrence Livermore National Laboratory
*Sandia National Laboratories
Livermore, CA 94551

Abstract

Lawrence Livermore, Sandia Livermore and Los Alamos National Laboratories have a joint project to develop an optimized hydrogen fueled engine for series hybrid automobiles. The major divisions of responsibility are: system analysis, engine design and kinetics modeling by LLNL; performance and emission testing, and friction reduction by SNL; computational fluid mechanics and combustion modeling by LANL. This project is a component of the Department of Energy, Office of Utility Technology, National Hydrogen Program. We report here on the progress on system analysis and preliminary engine testing. We have done system studies of series hybrid automobiles that approach the PNGV design goal of 34 km/liter (80 mpg), for 384 km (240 mi) and 608 km (380 mi) ranges. Our results indicate that such a vehicle appears feasible using an optimized hydrogen engine. The impact of various on-board storage options on fuel economy are evaluated.

Experiments with an available engine at the Sandia Combustion Research Facility demonstrated NO_x emissions of 10 to 20 ppm at an equivalence ratio of 0.4, rising to about 500 ppm at 0.5 equivalence ratio using neat hydrogen. Hybrid vehicle simulation studies indicate that exhaust NO_x concentrations must be less than 180 ppm to meet the 0.2 g/mile California Air Resources Board ULEV or Federal Tier II emissions regulations.

We have designed and fabricated a first generation optimized hydrogen engine head for use on an existing single cylinder Onan engine. This head currently features 14.8:1 compression ratio, dual ignition, water cooling, two valves and open quiescent combustion chamber to minimize heat transfer losses. Initial testing shows promise of achieving an indicated efficiency of 42 to 46% and emissions of less than 100 ppm NO_x. Hydrocarbons and CO are to be measured, but are expected to be very low since their only source is engine lubricating oil. A successful friction reduction program on the Onan engine should result in a brake thermal efficiency in excess of 40% compared to today's gasoline engines of 32%. Preliminary engine test data on indicated efficiency, MBT timing and burn duration are reported. Based on system studies requirements, the next generation engine will be about 2 liter displacement and is projected to achieve 46% brake thermal efficiency with outputs of 15 kW for cruise and 40 kW for hill climb. The concept of the series hybrid includes on/off engine operation mode with all operation taking place at wide open throttle to minimize pumping losses.

Introduction

Two recent developments have increased the interest in high fuel economy and low emission vehicles. High fuel economy vehicles, with up to 34 km/l (80 mpg), are one of the goals of the Partnership for a New Generation of Vehicles (PNGV); and the California Air Resources Board (CARB) has mandated the sale of low and zero emission vehicles.

Series hybrid vehicles appear to be a good solution for obtaining high fuel economy, low emission vehicles (Burke 1992, Smith 1993, Ross and Wu 1995). Series hybrid vehicles operate with an engine in an on-off mode.* The engine is turned on when it is necessary to charge a buffer storage system (flywheel, ultracapacitor, battery). When the storage is full, the engine is turned off, and all the energy is provided by the storage system. Series hybrid vehicles cannot transfer mechanical energy between the engine and the wheels. All the energy out of the engine is first converted to electrical energy, which is then used or stored according to the vehicle demands.

Considering the importance of the storage system, it is not surprising that series hybrid vehicles are very sensitive to the turnaround efficiency, power capacity, and energy storage capacity of the storage system. If minimum values of these parameters are not achieved, series hybrid vehicles lose their advantage with respect to parallel hybrid and conventional vehicles. Recent flywheel (Post et al. 1993) and ultracapacitor (Burke 1995) developments indicate optimism in reaching target performance values, which would make series hybrid vehicles the best choice for high fuel economy, low emission vehicles.

Series hybrid vehicles have a high efficiency because the engine operates mostly at the conditions that result in maximum vehicle fuel economy, without idling. When additional power is required during long hill climbs, the engine can be switched to a higher power level, trading off some fuel economy for the capacity of climbing long hills at higher speed. Series hybrid vehicles have low emissions because engine operation is not linked to vehicle driving conditions, therefore avoiding high emissions during hard accelerations. The energy level in the energy storage system can also be monitored for predicting the time for engine startup. This prediction can be used for preheating the catalytic converter, if this is required to reduce emissions.

This paper presents system analysis and hydrogen engine development work directed to obtaining a vehicle that approaches the 34 km/l (80 mpg) PNGV goal, and has very low emissions. Some of the vehicle and engine characteristics have been described in previous papers (Smith 1993; Smith 1994; Aceves and Smith 1995). The system analysis section of this paper shows a comparison between the hydrogen series hybrid (considering all the possible ways that can be used to store the hydrogen in the vehicle) and other technologies currently being considered for obtaining high fuel economy and low emissions. The engine development section of this paper gives a brief description of the engine characteristics, the expected engine performance, and the current status of the development work.

System Analysis

The system analysis presented in this paper uses HVEC, a vehicle evaluation code described in a previous publication (Aceves and Smith 1995). This code can be used to predict the fuel economy, range and performance of electric and series hybrid vehicles. In this paper, HVEC is

*On-off mode operation in a conventional drivetrain automobile during coast and stopped periods has recently been brought to the European market by Volkswagen in its Ecomatic automobile (Volkswagen 1994).

used to compare series hybrid vehicles with several combinations of fuels (gasoline, natural gas, diesel, methanol, hydrogen) and primary power supplies (piston engines, turbines, fuel cells), to evaluate which of these vehicles are most likely to meet the PNGV goal of 34 km/l (80 mpg, combined EPA driving cycle, 55% urban, 45% highway).

The vehicle comparison presented in this paper considers that it is possible to build a gasoline series hybrid having a 1000 kg empty weight and a 384 km (240 mi) range. This vehicle is then used as the base case for the comparison. The weight of other vehicle configurations is calculated from the base case vehicle by replacing the engine and fuel storage with alternative components, and calculating the differences in weight between the replaced components. It is also assumed that the chassis weight has to be increased by 0.3 kg for each kg of power train weight increase, due to the need for providing the required structural support.

The comparison between the different series hybrid vehicles is carried out under equal performance requirements. All vehicles analyzed in this paper have equal time for 0-97 km/h (60 mph) acceleration (10 s), equal hill climbing capacity (6% infinitely long hill at 97 km/h, or 60 mph) with a payload of 273 kg and equal range [either 384 km (240 mi) or 608 km (380 mi)]. Requiring equal performance implies that power train components (engine, motor, transmission) have different power output for each vehicle, as the power required to keep a desired performance increases as the vehicle weight increases. This constant performance requirement guarantees that all vehicles are being compared on equal terms. Other vehicle parameters, also considered equal for all vehicle configurations, are listed in Table 1.

Figure 1 shows a schematic of the vehicle configuration. Flywheels are used for energy storage in all vehicles, due to their high energy and power densities, and high turnaround efficiency. A detailed flywheel model has been incorporated into HVEC, which describes the measured performance of a flywheel which is currently in the prototype stage (Post et al. 1993). The model predicts flywheel turnaround efficiency and bearing losses as a function of flywheel state of charge and power.

Figure 2 shows the main results of the simulation and comparison of the series hybrid vehicles considered in this analysis. The figure shows lines of constant fuel economy (combined cycle) as a function of vehicle test weight and engine brake thermal efficiency. These contours have been generated by HVEC for vehicles with the desired constant performance parameters listed above. Figure 2 also shows points and regions, which indicate where the different series hybrid vehicles fall within the weight-efficiency diagram, for both the 384 km (240 mi) and the 608 km (380 mi) ranges. For some vehicles, the difference in weight for the two ranges being considered is very small. In these cases, only a point is indicated in the figure. A summary of the weights, engine efficiencies, and fuel economies for the series hybrid vehicles is listed in Table 2. Table 3 shows the weights of the hydrogen storage systems for the two ranges. Each of the vehicles is briefly described in the next section.

Vehicle Descriptions

Gasoline hybrid: This is the base-case vehicle, and it is assumed to have an empty weight of 1000 kg (1136 kg test weight) for a 384 km (240 mi) range. Engine efficiency is assumed to be 32 %, based on the peak efficiency of a current 9.5:1 compression ratio production engine (Thomson et al. 1987).

Gasoline hybrid, Lean-burn engine: This vehicle has a lean-burn (0.7 equivalence ratio) gasoline engine, which is assumed to have a 35% efficiency. Emission control for NO_x in this engine may require the use of a lean burn catalyst, still in the development stage. This vehicle is heavier than the previous, because lean-burn engines have a lower power output per unit of displacement than stoichiometric engines. Hence to maintain the required performance the engine must be bigger and heavier which also adds slightly to the chassis weight as described above.

Diesel hybrid: The efficiency for the diesel engine is assumed to be 46%, based on a recent production truck engine (Tsujita et al. 1993). However, small diesel engine efficiencies can be substantially lower than this (Lawrence and Evans 1990). A region is shown in Fig. 2, which indicates the possible efficiency of current and future small diesel engines.

Compressed Natural Gas (CNG) hybrid: Due to the higher effective octane number, CNG engines can operate at a high (12:1) compression ratio, and therefore their efficiency can be higher than the efficiency of gasoline engines.

CNG hybrid, Lean-burn: CNG engines operating lean are assumed to have a 38% efficiency. This vehicle is slightly heavier than the previous, due to the extra weight of the lean engine.

Gas turbine hybrid: Gas turbines are expected to be lighter than any other engine. However, their efficiency is relatively low, due to the limit in maximum temperature that the turbine materials can withstand. A 32% turbine efficiency is assumed here for automotive turbines. However, an area is indicated in Fig. 2, extending to a maximum efficiency of about 40%, which has been recently set as a PNGV goal (PNGV 1995), and may be possible in the future with high temperature turbines.

Hydrogen Fueled Vehicles

Hydrogen hybrid, Cryogenic liquid hydrogen storage: This vehicle operates with an optimized hydrogen engine, that is expected to have a 46% brake thermal efficiency (see the Engine Development section of this paper for a description). The engine operates at a very high compression ratio (15:1), very lean (0.4 equivalence ratio), and is therefore substantially heavier than a stoichiometric engine. The cryogenic liquid storage has a reasonable weight and volume, and has a proven record of safety (Peschka 1992).

Hydrogen hybrid, Iron-titanium hydride storage: Iron-titanium hydride is a very safe way to store hydrogen with a very low energy penalty for compressing or liquefying (Buchner 1977). The storage system also has a reasonable volume. The major drawback of hydride storage is the high system weight. The mileage penalty is 10 mpg for the nearly 400 kg vehicle weight increase over the liquid hydrogen hybrid.

Hydrogen hybrid, Magnesium hydride storage: Magnesium hydrides are lighter than iron-titanium hydrides. However, they require high temperature thermal energy for releasing the hydrogen. Exhaust gases emitted by the optimized hydrogen engine have a low temperature (~300°C). Therefore, it is necessary to burn some of the hydrogen fuel to desorb the hydrogen contained in the hydride. This reduces the engine-storage system efficiency to about 40 % (Handrock 1995).

Hydrogen hybrid, Pressure storage at 3600 psi: This system has a low weight, but a very high volume (about 300 liters for a 608 km range), which may rule out this form of storage for automobiles. The volume can be reduced by using higher pressure containers. However, cost and safety issues still have to be addressed for very high pressure tanks.

Hydrogen hybrid, Methanol and reformer: This vehicle is fueled by methanol, avoiding therefore many of the direct infrastructure problems associated with hydrogen. Methanol is reformed on board, and converted into hydrogen and carbon monoxide, which are then burned in the engine. The transformation of methanol does not introduce any energy losses if exhaust energy is used for the process [energy gains may even occur (Pettersson and Sjostrom 1991)]. An on-board reformer introduces a weight penalty. However, the system volume is acceptable (estimated at 120 liters, including the methanol tank).

Hydrogen-methane hybrid, Pressure storage at 3600 psi: This vehicle is fueled with a 50%-50% molar mixture of methane and hydrogen. The presence of hydrogen in the mixture allows the engine to operate very lean, while the presence of methane results in an acceptable volume for the pressure storage (150 liters for 608 km range). The efficiency of the engine is assumed to be slightly lower than the efficiency for the pure hydrogen engine, because the presence of higher hydrocarbons in the methane may limit the compression ratio to avoid engine knock.

Proton Exchange Membrane (PEM) fuel cell hybrid, Cryogenic liquid hydrogen storage: Fuel cell efficiency and weight are obtained from a recent publication (Allison 1993). This vehicle has the highest fuel economy of all vehicles being compared. A fuel cell region is also shown in Fig. 2 to indicate the possibility of future improvements.

System Analysis Summary

Figure 2 shows that the lines of constant fuel economy have a small slope, indicating that mass does not have a great effect on fuel economy (34 kg of weight reduction are necessary for a 1 mpg increase in fuel economy). This indicates that, in reaching the 34 km/l (80 mpg) PNGV goal, it is more important to achieve a high engine fuel economy than a low vehicle mass. Figure 2 also shows that turbines, CNG engines and gasoline engines are unlikely to achieve the PNGV goal in a vehicle with the characteristics considered in this paper. Diesels, hydrogen engines, and fuel cells remain as the three technologies that have the possibility of reaching the PNGV goal. However, these have other limitations that may restrict their access to the market. The main difficulty with diesel engines is meeting the emission requirements for NOx and particulate matter. Hydrogen vehicles can achieve very low emissions, but the need for a hydrogen infrastructure may limit their extended use. Hydrogen storage is also a problem. Fuel cells are currently bulky, heavy, and very expensive. Many of the existing fuel cells are fueled with hydrogen, and therefore have the same infrastructure and storage problems as hydrogen engine vehicles. Solving satisfactorily the problems associated with either one of these technologies will result in an efficient, low emission car that may reduce oil imports and urban pollution. At the present time, hydrogen engine vehicles appear to be the most likely to meet all the requirements, since the storage and infrastructure issues can be solved with current technology at a reasonable cost, as shown in this and in a recent publication (Berry et al. 1994).

Optimized Hydrogen Engine Development

Emissions

The major emissions from hydrogen-fueled engines are NO_x which consists of NO (nitric oxide) and NO_2 (nitrogen dioxide). These can be considerably higher than the NO_x emissions from conventional gasoline-fueled engines due to its higher adiabatic flame temperature. High NO_x emissions are the result of high combustion temperatures in the burned gases, which occur when engines are operated at or near stoichiometric fuel-air ratios. In stoichiometric spark-ignition engines, NO usually represents 98% or more of the NO_x, while in compression ignition engines (diesels) NO exceeds 90% only at high loads or high speeds. An excellent discussion of the detailed chemical kinetic mechanisms of the NO formation process can be found in the literature (Heywood 1988).

To reduce combustion temperatures, and hence NO_x, the fuel-air ratio is reduced, which dilutes the combustion products with air. It is also possible to achieve similar results by recirculating exhaust gases (EGR) to dilute the hot products (Ibid.). However, as the equivalence ratio is decreased, flame speed decreases until unstable (incomplete or late) combustion precludes further leaning. In extreme cases the flame speed is so low that combustion is not completed before the exhaust valve opens. In some situations, turbulent gas motion mixes the flame front with products and the flame is quenched. This occurs at an equivalence ratio of about 0.65 when using hydrocarbon fuels. Fortunately, hydrogen has a unique property that allows it to be burned at significantly lower temperatures than any other fuel: its high flame speed. A comparison of the laminar flame speeds of hydrogen, gasoline methanol reformate, a hydrogen/CNG blend, and methane are shown in Fig. 3. Note that flame speeds comparable to the lower equivalence ratio limits for methane and gasoline (about 0.65) are in the region of 0.3 for hydrogen. The flame speed in an engine is much higher than the laminar flame speed because of turbulence. Turbulence and burned gas expansion act as multipliers on the laminar flame speed.

The extensive work of Homan (Homan 1978) on direct injection of hydrogen in a CFR (Cooperative Fuels Research) engine operated in both the spark-ignition and compression ignition modes indicates that late injection always results in one to two orders of magnitude more NO_x production than does lean, premixed, spark-ignited operation. Thus it does not appear promising to consider diesel cycles when trying to minimize NO_x production. Homan measured 0.005 g of NO_x per kWh of work produced using a spark-ignited hydrogen air mixture at equivalence ratio 0.38 (Ibid.). Das (Das 1990) measured the NO_x emissions from another hydrogen-fueled research engine as a function of equivalence ratio at compression ratios up to 11:1 and are consistent with the extensive measurements of Swain in an 8.5:1 CR engine (Swain et al. 1983). Figure 4 shows measurements made by this project on a Sandia CLR (Council for Lubricating Research) engine which are in agreement with the literature values of Swain and Das.

Operation at premixed equivalence ratios that are too low will result in unburned hydrogen that can form hydrogen peroxide within the combustion chamber. Hydrogen peroxide emissions could act as a source of hydroxyl radicals to promote photochemical smog. Sinclair and Wallace (Sinclair and Wallace 1984) found that hydrogen peroxide levels rose as the equivalence ratio was reduced below 0.4. At low hydrogen peroxide levels, passage of the exhaust through a conventional tailpipe and muffler resulted in greatly reduced peroxide levels. They state that a high-surface-area exhaust system would easily decompose the hydrogen peroxide on the metal walls to negligible levels. Even so, hydrogen peroxide emissions will put a lower limit on useful equivalence ratio.

Hydrogen engines emit small quantities of hydrocarbons (HC) and carbon monoxide (CO) from the decomposition and partial oxidation of the lubricants left on the cylinder walls by piston rings and from the valve guides. The exact HC and CO levels produced are probably very dependent on the detailed engine design. However, it is possible to get what is probably an upper bound on these emissions from recent measurements made on a large two-stroke diesel engine that was run on hydrogen (Hedrick 1993). The average of the "11 Mode Emission Test" gave HC of 0.010 g/kWh and CO of 0.0176 g/kWh in the 9.05 liter displacement engine. These are probably upper bounds because this two-stroke diesel sweeps the piston rings across the intake ports, which is likely to cause more oil to be transported into the combustion chamber by the passage of intake air.

There is a considerable body of knowledge on how the design details of piston rings affects oil transport into the combustion chamber (McGeehan 1979). Experiments by Furuhama, Hiruma, and Enomoto (Furuhama et al. 1978) with a three-piece oil ring reduced HC by nearly a factor of two in a liquid-hydrogen-fueled premixed engine. These researchers also removed the chamfer from the upper piston rings, which reduced blowby by a factor of four. Thus, with attention to the design issues of lubricant contributions to hydrogen engine emissions and with the current knowledge of the emission causes, it should be possible to keep the HC and CO emissions extremely low.

It is interesting to note that the tests done (Hedrick 1993) determined a NO_x emission of 0.575 g/kWh for the diesel. This is more than 100 times the value measured by Homan in the premixed spark-ignition case. This again supports the conclusion that diesel operation of hydrogen engines is not likely to have tolerable NO_x emissions. However, there is the possibility of using very large amounts of EGR to reduce temperatures and NO_x production in diesels.

Thus the literature gives clear guidance that an optimized hydrogen engine that minimizes emissions should operate as a premixed homogeneous-charge, spark-ignition engine at an equivalence ratio of about 0.4, and that attention in its design should be given to limiting lubricant contributions to the emissions. Note that the low emissions achievable in this type of engine do not require a catalyst.

Efficiency

There are two primary reasons to optimize a hydrogen engine for maximum efficiency. First, on-board hydrogen storage is a difficult task for automotive applications and, second, the cost of hydrogen on an energy content basis will likely remain higher than gasoline for the next several decades. The automotive storage problem is discussed in some detail by Robinson and Handrock (Robinson and Handrock 1994). The cost of hydrogen depends not only on hydrogen production costs but also on the distribution and bulk storage systems used. These infrastructure issues are addressed (Berry et al. 1994).

The thermal efficiency as a function of compression ratio for a number of single-cylinder research engine experiments on hydrogen is shown in Fig. 5. Indicated efficiency is more appropriate to report for single-cylinder research engines (net work done on the piston), because the high friction of most research engines is not representative of modern multi-cylinder engines.

Included in Fig. 5 is a plot of:

$$\eta = 1 - [1/(R_c)^{\gamma-1}] \tag{1}$$

the Otto cycle indicated thermal efficiency for constant ratio of specific heats. R_c is the compression ratio and γ is the ratio of specific heats, taken here to be 1.3. The indicated efficiency data by King (King et al. 1958) is for the most part below the ideal indicated efficiency. A hint as to the possible cause for the rolloff in efficiency measured by King et al., is given by the work of Caris and Nelson (Caris and Nelson 1959), who achieved 44.5% indicated thermal efficiency at 17:1 compression ratio using highly leaded gasoline at an equivalence ratio of 0.93. Their experiment, like virtually all of the engine compression ratio variation experiments, reduced the clearance height (the distance between the top of the piston and the head) as the compression ratio was raised. Thus at low compression ratios the surface-area-to-volume ratio of the combustion chamber at Top Dead Center (TDC) is low, and at high compression ratios the surface to volume ratio is high. This can have a major effect on heat losses from the burned gas. Heywood states that the boundary layer during expansion is of the order of 2 to 3 mm (Heywood 1988) and that because it is cooler than the core gases, it contains the majority of the mass in the cylinder if the surface-to-volume ratio is high. This effect has been highlighted in a recent engine model that compared well with production engines of varying surface-to-volume ratios (Muranaka et al. 1987). Based on the dimensions supplied in King's work on a modified CFR engine, it is estimated that the clearance height at TDC was 8 mm at 12:1 compression ratio and only 4.6 mm at 20:1. Thus at the higher compression ratios there is little or no unaffected (uniform high temperature) core gases — virtually all the mass is in the cooling boundary layer. This is supported by Fig. 6, where the difference between the ideal thermal efficiency calculated from Eq. (1) and the measured indicated thermal efficiency of King et al., Oehmichen (Oehmichen 1942), and Mathur (Mathur and Khajuria 1984) are plotted against the surface-to-volume ratio which has been estimated from the engine schematic and dimensions provided in their papers. (Figures 5 and 6 also include preliminary data from the Onan experiment and are discussed later.)

Thus heat transfer losses are likely to be the main reason for experiments to fall well short of the ideal efficiency. It is noted that "timing losses" also contribute to less than ideal performance since the heat addition is not at constant volume due to the finite time it takes for the charge to burn. However, as Muranaka et al. show this loss is small if the burn duration is less than 50 to 60 crank angle degrees. This is further supported in Fig. 6 by the comparison of King's 1200 rpm data with the 1800 rpm data, which shows slightly greater than 50% increase in losses. This is what would be expected because the time for heat transfer to take place is inversely proportional to engine speed, and the equivalence ratio for the lower-speed case is a bit higher than the 1800 rpm case. The effects of heat transfer losses (Muranaka et al. 1987) for stoichiometric gasoline engines can be reasonably well fit by:

$$Q_c/Q_f = 20\ (1400/N)^{0.5} \qquad (2)$$

where Q_c/Q_f is the fraction of energy of the fuel lost in percent and N is engine rpm. This fit of the model output is for wide open throttle.

Thus an optimized engine should have a compact combustion chamber to minimize heat losses if it is to be successful. Using a conventional engine and merely raising the compression ratio by reducing the clearance height is not likely to give acceptable results. This implies a longer stroke engine, which raises issues about friction.

Care must also be exercised in the design of an optimized engine that friction does not reduce the output excessively. Since constant-speed, constant-load is the requirement for hybrid applications, there is an opportunity to reduce friction because intermittent high-speed operation is necessary only for hill climb. In addition, by matching the engine to its load (the electrical generator) accurately, only wide-open throttle operation is required. Thus pumping losses can be minimized, and the engine intake and exhaust system can be tuned for maximum volumetric efficiency. Such tuning could compensate for the nearly 12% loss in volumetric efficiency that occurs by operating at an equivalence ratio of 0.4 because of the volumetric displacement of air by hydrogen.

Engine friction rises rapidly with speed. A correlation of friction (in bars of pressure) for four-stroke engines in the range of 0.85 to 2 liter displacement was found by Barnes-Moss (Barnes-Moss 1975) as:

$$\text{fmep (bar)} = 0.97 + 0.15(N/1000) + 0.05(N/1000)^2, \qquad (3)$$

where fmep is friction mean effective pressure, and N is the rpm. This fit is in good agreement with data in the range of 1000 to 5000 rpm and was done for wide-open throttle. Thus there is a compromise that must be made in engine speed between friction rising with engine speed and heat losses dropping with increasing engine speed. Since the fraction of work lost to friction depends on the indicated mean effective pressure, it is not possible to predict analytically the optimum engine speed. However, it is likely that the ideal speed will be between 1500 and 3000 rpm. Therefore, optimized hydrogen engines probably will not be high-speed engines.

Although the points cited here about engine efficiency are encouraging for achieving brake thermal efficiencies in the mid-to-upper 40% range, low equivalence ratio and low speed will mean low power output for a given displacement. The displacement required for the projected need of about 40 kW (54 hp) for the hybrid vehicle application will probably require a 2.0 liter engine in a four-stroke version. A modern gasoline engine can produce 100 to 110 kW from a 2.0 liter displacement engine. The impact of turbocharging to raise specific output and indicated mean effective pressure needs to be considered. Alternatively, the problems of engine oil contributing to emissions in a two-stroke version may have to be addressed if the four-stroke engine is too large for integration into a low-aerodynamic-drag automobile. Combustion and engine models can guide our choices of the parameters for an optimized engine, but only experimental data can confirm our goals.

Engine Development Summary

From a review of the available experiments on hydrogen engines, the following conclusions are drawn:

- Low emissions can be achieved without a catalyst if a hydrogen engine is operated at an equivalence ratio between 0.3 and 0.5. The lower bound is controlled by rising hydrogen peroxide production, while the upper bound is controlled by NO_x production. In addition, the engine design should minimize lubricant contributions to the combustion chamber.

- High efficiency in an optimized hydrogen engine is likely to be achieved if:
  1. A compact chamber with low surface-to-volume ratio is used to minimize heat losses to the walls.
  2. Mechanical friction is minimized for the constant-speed/load conditions.
  3. High volumetric efficiency is achieved through intake and exhaust tuning techniques to maximize the indicated mean effective pressure and engine output relative to mechanical friction.

- Optimum engine speed cannot be accurately predicted but will be relatively low.

- Specific power output will be relatively low and may require either turbocharging or consideration of two-stroke operation.

Current Engine Development Status

We have designed and fabricated a cylinder head for an existing Sandia Onan engine. This engine was originally a small, single cylinder diesel. The new head draws upon our understanding of the literature implications on NO_x emissions and efficiency. It also incorporates many of the suggestions by Professor Mike Swain to minimize oil intrusion into the combustion chamber. The design includes dual ignition from spark plugs located to minimize the flame travel distance for low cyclic variation at very low equivalence ratios. This will compensate for the low flame speed of lean operation. The design uses a low turbulence right circular cylinder shaped combustion chamber to minimize heat loss. Details of this first attempt at an optimized engine are given in Table 4.

The choice of chamber shape appears to be the best based on the recent work of the Lund Institute (Johansson and Olsson 1995) where ten chamber shapes were compared at 12:1 compression ratio. Using CNG at an equivalence ratio of a 0.67, they achieved 49% indicated efficiency. The Onan design uses 14.8:1 compression ratio to achieve high efficiency, but has higher surface to volume ratio than the Lund Institute experiments.

Preliminary measurements, as shown in Fig. 7, yield 42 to 46% indicated efficiency on the Onan experiments. These values have also been shown in figures 5 and 6 for comparison to previous work. The lower indicated efficiency value is computed from the cylinder pressure data taken via the AVL model XX water cooled transducer while the higher values use the motoring method that used a BBBXXX torque tranducer. It has been shown (Kerley and Thurston, 1962) that the pressure method gives a lower indicated efficiency than the motored by 1.5 to 2% in the 10:1 to 14:1 compression range. The preliminary experimental differences in the two methods of determining indicated efficiency are 3 to 5%. One potential explanation for the lower than expected indicated efficiency is that the particular combination of intake runner arrangement and no intentional swirl has accidentally resulted in much greater turbulence than desired. Such an explanation is supported by the relatively fast burn observed even at 1200 rpm which requires 16 degrees of advance for MBT (minimum advance for best torque) at an equivalence ratio of 0.35 and only 10 degrees required at 0.46 equivalence ratio.

The authors remain hopeful that higher volumetric efficiency and higher engine speeds will result in higher efficiencies. The surface to volume ratio in the Onan experiment is limited by the engine stroke which will be changed in the next generation engine for improved efficiency.

Acknowledgments

The authors acknowledge contributions by Professor Michael Swain of the University of Miami on engine design and the contributions of Messieurs Luis Bernardeaz and Jim Boehmke of Sandia/California in experiment hardware development. Also the contributions of Dr. Robert M. Green of Sandia/California for the CLR engine experiment on NO_x. This work was performed under the auspices of the U.S. Department of Energy by the Lawrence Livermore National Laboratory under Contract No. W-7405-ENG-48.

References

Aceves, S.M., and J.R. Smith, 1995, "A Hybrid Vehicle Evaluation Code and Its Application to Vehicle Design," SAE paper 950491.

Allison Gas Turbine Division, GM Corp., 1993, "Research and Development of Proton Exchange Membrane (PEM) Fuel Cell system for Transportation Applications, Initial Conceptual Design Report," report EDR 16/94, prepared for the Office of Transportation Technologies, Department of Energy.

Berry, G.D., A.D. Pasternak, G.D. Rambach, J.R. Smith and R.N. Schock, 1994, "Hydrogen as a Future Transportation Fuel," Lawrence Livermore National Laboratory report no. UCRL-JC-117945.

Barnes-Moss, H.W., 1975, "A Designer's Viewpoint," Passenger Car Engines Conference Proceedings, Institution of Mechanical Engineers, London, pp. 133-147.

Buchner, H., 1977, "The hydrogen/Hydride Energy Concept," in Andresen and Maeland, editors: "Hydride for energy Storage," Pergamon Press.

Burke, A.F., 1992, "Hybrid/Electric Vehicle Design Options and Evaluations," SAE paper 920447.

Burke, A.F., 1995, "The Potential of Electrochemical Capacitors for Electric and Hybrid Vehicle Applications," Proceedings of the Workshop Basic Research Needs for Vehicles of the Future," New Orleans, LA

Caris D.F., and E.E. Nelson, 1959, "A New Look at High Compression Engines," *Society of Automotive Engineers Transactions*, Vol. 67, pp. 112-124.

Das, L.M., 1990, "Hydrogen Engines: A View of the Past and a Look into the Future," *International Journal of Hydrogen Energy*, Vol. 15, No. 6, pp. 425-443.

Furuhama, S., M. Hiruma and Y. Enomoto, 1978, "Development of a Liquid Hydrogen Car," *International Journal of Hydrogen Energy*, Vol. 3, pp 61-81.

Handrock, J., 1995, personal communication, Sandia/California, Livermore, CA.

Hedrick, J.C., 1993, "Advanced Hydrogen Utilization Technology Demonstration," Southwest Research, Inc., Final Report, Project No. 03-5080.

Heywood, J.B., 1988, *Internal Combustion Engine Fundamentals*, McGraw-Hill, New York, Ch 11.

Heywood, J.B., *Internal Combustion Engine Fundamentals*, p. 697.

Homan, H.S., "An Experimental Study of Reciprocating Internal Combustion Engines Operated on Hydrogen," PhD thesis, Cornell University, January 1978, p. 69.

Johansson, B., and K. Olsson, 1995, "Combustion chambers for National Gas SI Engines Part I: Fluid Flow and Combustion," SAE paper 950469.

Kerley, R. V. and Thurston, K. W., "The Indicated Performance of Otto-Cycle Engines," *SAE Transactions*, Vol. 70, pp. 5-37, 1962.

King, R.O., S.V. Hayes, A.B. Allan, R.W.P. Anderson, and E.J. Walker, "The Hydrogen Engine: Combustion Knock and the Related Flame Velocity," *Transactions of the Engineering Institute of Canada*, Vol. 2, No. 4, December 1958.

Lawrence, R.J, and R.W. Evans, 1990, "The Ford 1.8L Four Cylinder Turbocharged Diesel Engine for Passenger Car Application," SAE paper 901716.

Mathur, H.B., and P.R. Khajuria, 1984, "Performance and Emission Characteristics of Hydrogen Fueled Spark Ignition Engine," International Journal of Hydrogen Energy, Vol. 9, pp. 729-735.

McGeehan, J.A., 1979, "A Survey of the Mechanical Design Factors Affecting Engine Oil Consumption," *Society of Automotive Engineers Transactions*, Vol. 88, SAE paper 790864.

Muranaka, S., Y. Takagi and T. Ishida, 1987, "Factors Limiting the Improvement in Thermal Efficiency of S. I. Engine at Higher Compression Ratio," *Society of Automotive Engineers Transactions*, SAE paper 870548.

Oemichen, M., 1942, "Hydrogen as an Engine Fuel," Engine Laboratory of the Technische Hochschule, Dresden, Germany, VDI-Verlag GmbH, Berlin NW, V.D.I. Paper No. 68.

Peschka, W., 1992, "Liquid Hydrogen: Fuel of the Future," Springer-Verlag, New York.

Pettersson, L. and K. Sjostrom, 1991, "Decomposed Methanol as a Fuel - A Review," Combustion Science and Technology, Vol. 80, pp 265-303.

PNGV, 1995, "Inventions Needed for PNGV," U.S. Department of Commerce, Washington, DC.

Post, R.F., T.K. Fowler, and S.F. Post, March 1993, "High Efficiency Electromechanical Battery," *Proceedings of the IEEE*, Vol. 81, No. 3.

Robinson S.L., and J.L. Handrock, February 1994, "Hydrogen Storage for Vehicular Applications: Technology Status and Key Development Areas," Sandia National Laboratories White Paper, Livermore, CA.

Ross, M., and W. Wu, 1995, "Fuel Economy Analysis for a Hybrid Concept Car Based on a Buffered Fuel-Engine Operating at a Optimal Point," SAE paper 950958.

Sinclair L.A., and J.S. Wallace, 1984, "Lean Limit Emissions of Hydrogen-Fueled Engines," *International Journal of Hydrogen Energy*, Vol. 9, No. 1/2, 00. pp. 123-128.

Smith, J.R., 1993, "The Hydrogen Hybrid Option," Proceedings of the Workshop on Advanced Components for Electric and Hybrid Electric Vehicles, Gaithersburg, MD, NIST special publication 860.

Smith, J.R., "Optimized Hydrogen Piston Engines," SAE's Convergence'94, Detroit, MI, October 18, 1994, Lawrence Livermore National Laboratory Report No. UCRL-JC-116894..

Swain, M.R., R.R. Adt, Jr., and J.M. Pappas, May 1983, *Experimental Hydrogen-Fueled Automotive Engine Design Data-Base Project,* Vol. 1, DOE Contract No. E(04-3)-1212, p. 20.

Thomson, M.W., A.R. Frelund, M. Pallas, and K.D. Miller, 1987, "General Motors 2.3L Quad 4 Engine," SAE paper 870353.

Tsujita, M., S. Niino, T. Ishizuka, A. Kakinai, and A. Sato, "Advanced Fuel Economy in Hino New PIIC Turbocharged and Charge-Cooled Heavy Duty Diesel Engine," SAE paper 930272.

Volkswagen, 1994, "Green VW," Vehicle News, Number 211, November/December, pp. 196-199.

Table 1. Parameters common to all vehicle configurations being analyzed.

Frontal area, m^2	2.04
Aerodynamic drag coefficient	0.24
Coefficient of rolling friction	0.007
Transmission efficiency (single speed transmission)	0.95
Flywheel energy storage capacity, kWh	1.0
Flywheel maximum power output, kW	100.0
Generator efficiency	0.95
Accessory load, W	1000

Table 2. Engine efficiencies, weights and combined cycle (55% urban, 45% highway) fuel economies for the vehicles being compared in the paper. All vehicles have the same performance parameters. Two vehicle ranges are considered: 384 km (240 mi) and 608 km (380 mi). Overall test weights assume a 136 kg pay load which is added to the empty weight.

Vehicle description	Engine efficiency, %	Test weight, kg		Fuel economy km/l (mpg)	
		384 km	608 km	384 km	608 km
Gasoline hybrid, stoichiometric engine	32	1136	1146	25(58)	25(58)
Gasoline hybrid, lean-burn engine	35	1174	1183	27(63)	27(63)
Diesel hybrid	46	1148	1158	35(83)	35(83)
CNG hybrid, stoichiometric engine	35	1137	1152	27(64)	27(64)
CNG hybrid, lean-burn engine	38	1174	1188	29(69)	29(69)
Gas turbine hybrid	34	1105	1115	26(62)	26(62)
Hydrogen hybrid, cryogenic liquid storage	46	1218	1247	34(81)	34(80)
Hydrogen hybrid, Fe-Ti hydride storage	46	1479	1643	31(74)	30(70)
Hydrogen hybrid Mg hydride storage	40[1]	1409	1514	28(66)	27(63)
Hydrogen hybrid, 3600 psi pressure storage	46	1239	1262	34(80)	34(79)
Hydrogen hybrid, methanol and reformer	46	1283	1302	34(79)	33(78)
Hydrogen-methane hybrid 3600 psi pressure storage	45	1226	1242	34(79)	339(78)
PEM fuel cell hybrid, cryogenic liquid H_2 storage	47[2]	1171	1192	36(85)	36(84)

[1] This value takes into account the amount of hydrogen that is necessary to burn to extract the hydrogen from the storage.

[2] Fuel cells do not require a generator, therefore, "engine efficiency" for a fuel cell is given as the fuel cell efficiency divided by the generator efficiency (95%), to allow a direct comparison with engine efficiencies.

Table 3. Empty weights in kilograms for hydrogen storage systems, for the two ranges being considered.

	384 km range	608 km range
Cryogenic liquid	25	39
FE - Ti hydride	202	321
Mg Hydride	153	232
3600 psi	35	47
Methanol and reformer	46	48
Hydrogen-methane 50/50 @3600 psi	21	28

Table 4. Modified Onan research engine specifications.

Displacement	493 cm^3
Bore	82.55 mm
Stroke	92.075 mm
Bore to stroke ratio	0.90
Compression ratio (initial)	14.8:1
Intake and exhaust valve diameters	34.6 mm
Spark plug location from centerline	20.6 mm (2 each)

Figure Captions

1. Series hybrid drivetrain schematic.

2. A comparison of series hybrid automobiles with equal acceleration, hill climb capability and range. Open symbols are for 240 mile range, filled symbols are for 380 mile range.

3. Comparison of the laminar flame speed of hydrogen (data compiled by Marinov, LLNL) with that of methane, gasoline (Heywood 1988), methanol reformate and a hydrogen/CNG blend.

4. Based on recent Sandia experiments in a CLR research engine, NOx decreases dramatically as a hydrogen engine is leaned below 0.5 equivalence ratio.

5. Thermal efficiency of various hydrogen-fueled research engines compared with ideal indicated efficiency.

6. Efficiency loss (ideal minus indicated) versus estimated surface-to-volume ratio in King et al., Oehmichen and Mathur experiments on a hydrogen engines. Preliminary and predicted data for the Onan experiment are also shown.

7. Preliminary indicated thermal efficiency by pressure integration and motoring methods.

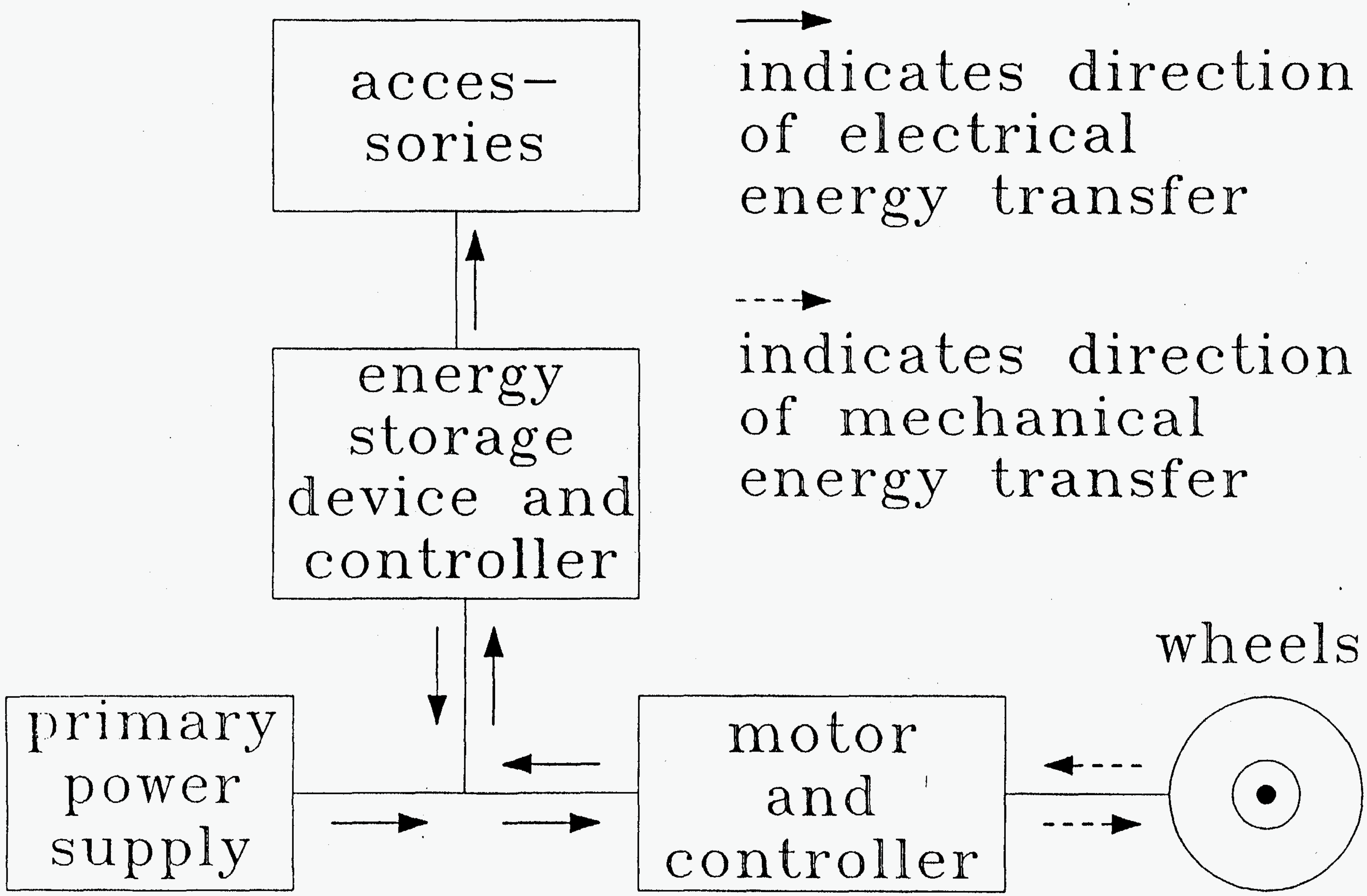

acces-
sories
energy
storage
device and
controller
primary
power
supply
motor
and
controller
wheels
indicates direction
of electrical
energy transfer
indicates direction
of mechanical
energy transfer

Fig 1

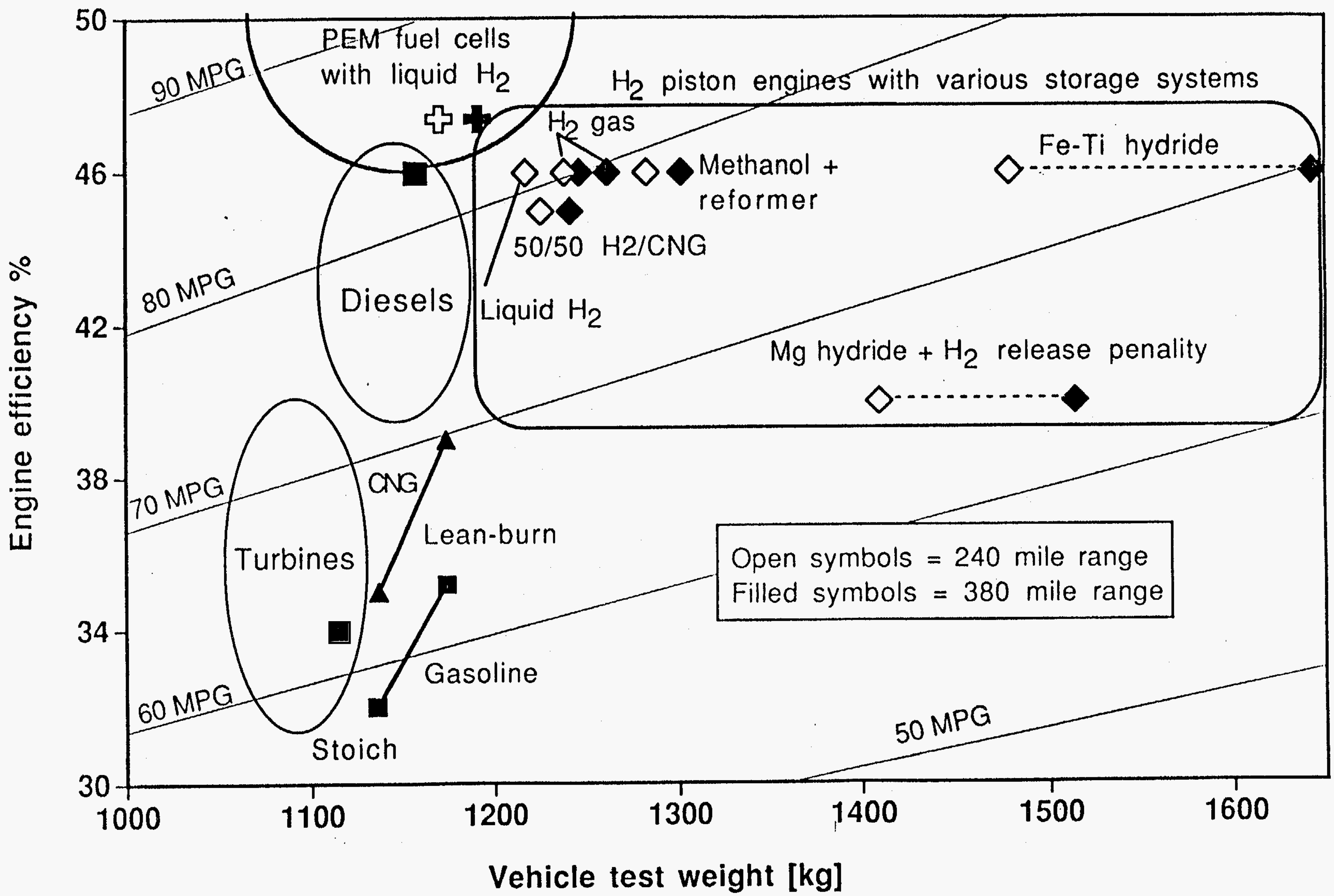

PEM fuel cells with liquid H2
90 MPG
80 MPG
70 MPG
60 MPG
50 MPG
H2 piston engines with various storage systems
H2 gas
Methanol + reformer
Fe-Ti hydride
50/50 H2/CNG
Liquid H2
Diesels
Mg hydride + H2 release penality
CNG
Lean-burn
Turbines
Gasoline
Stoich
Open symbols = 240 mile range
Filled symbols = 380 mile range
Engine efficiency %
Vehicle test weight [kg]
50
46
42
38
34
30
1000
1100
1200
1300
1400
1500
1600

Figure 2

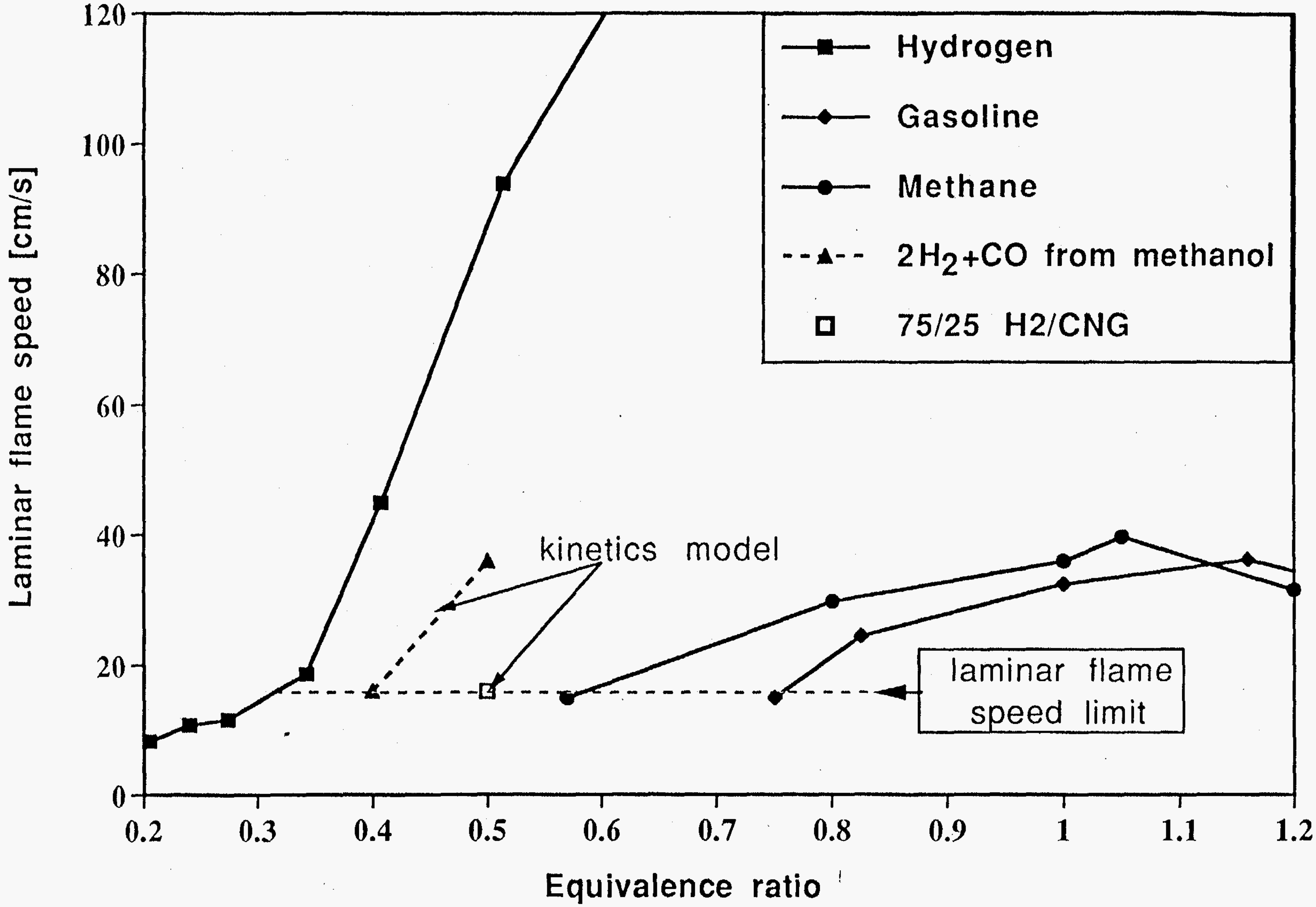
Hydrogen
Gasoline
Methane
2H2+CO from methanol
75/25 H2/CNG
kinetics model
laminar flame speed limit
Laminar flame speed [cm/s]
Equivalence ratio
0
20
40
60
80
100
120
0.2
0.3
0.4
0.5
0.6
0.7
0.8
0.9
1
1.1
1.2

Figure 3

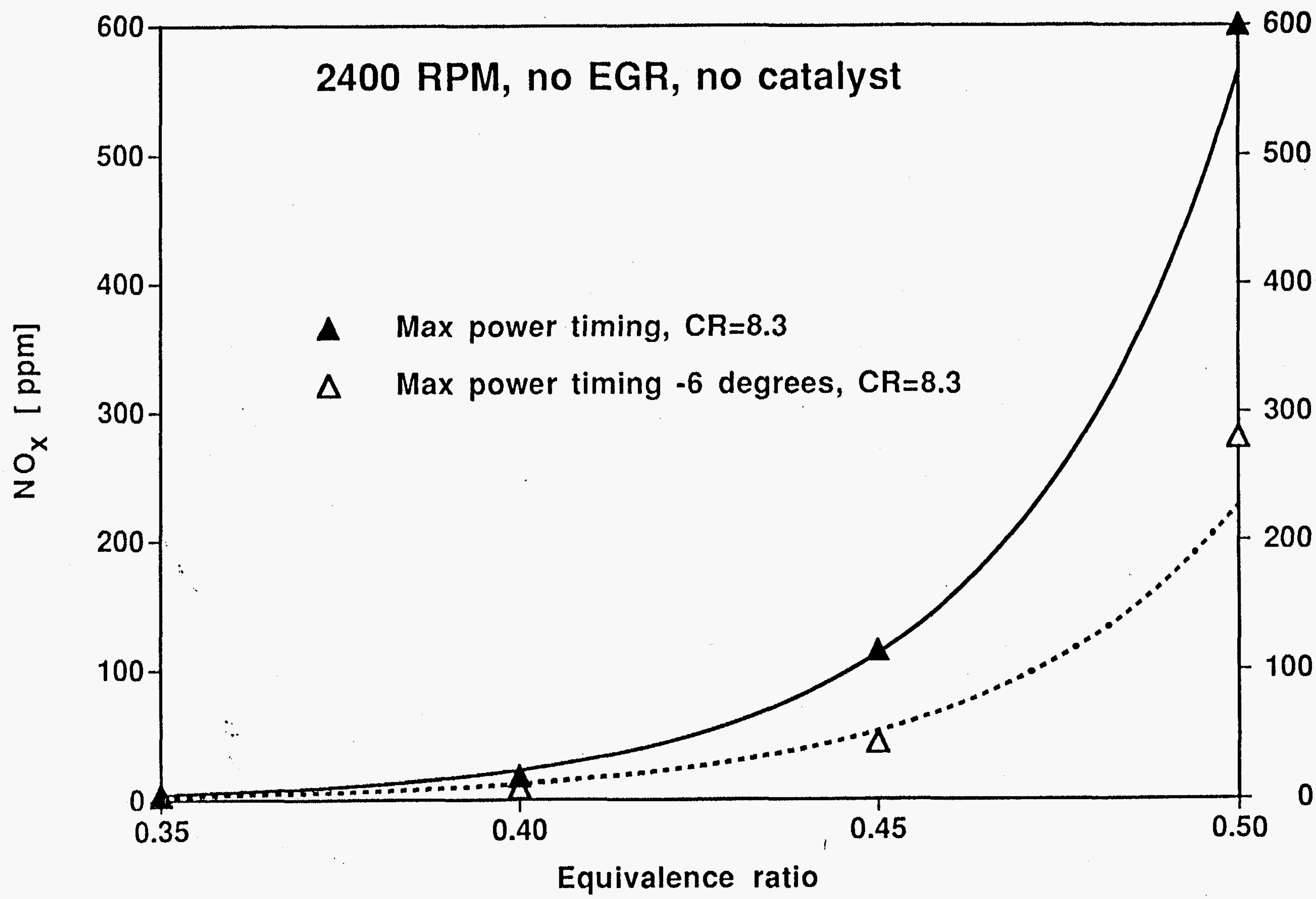
2400 RPM, no EGR, no catalyst
Max power timing, CR=8.3
Max power timing -6 degrees, CR=8.3
NOx [ppm]
Equivalence ratio
0
100
200
300
400
500
600
0.35
0.40
0.45
0.50

Figure 4

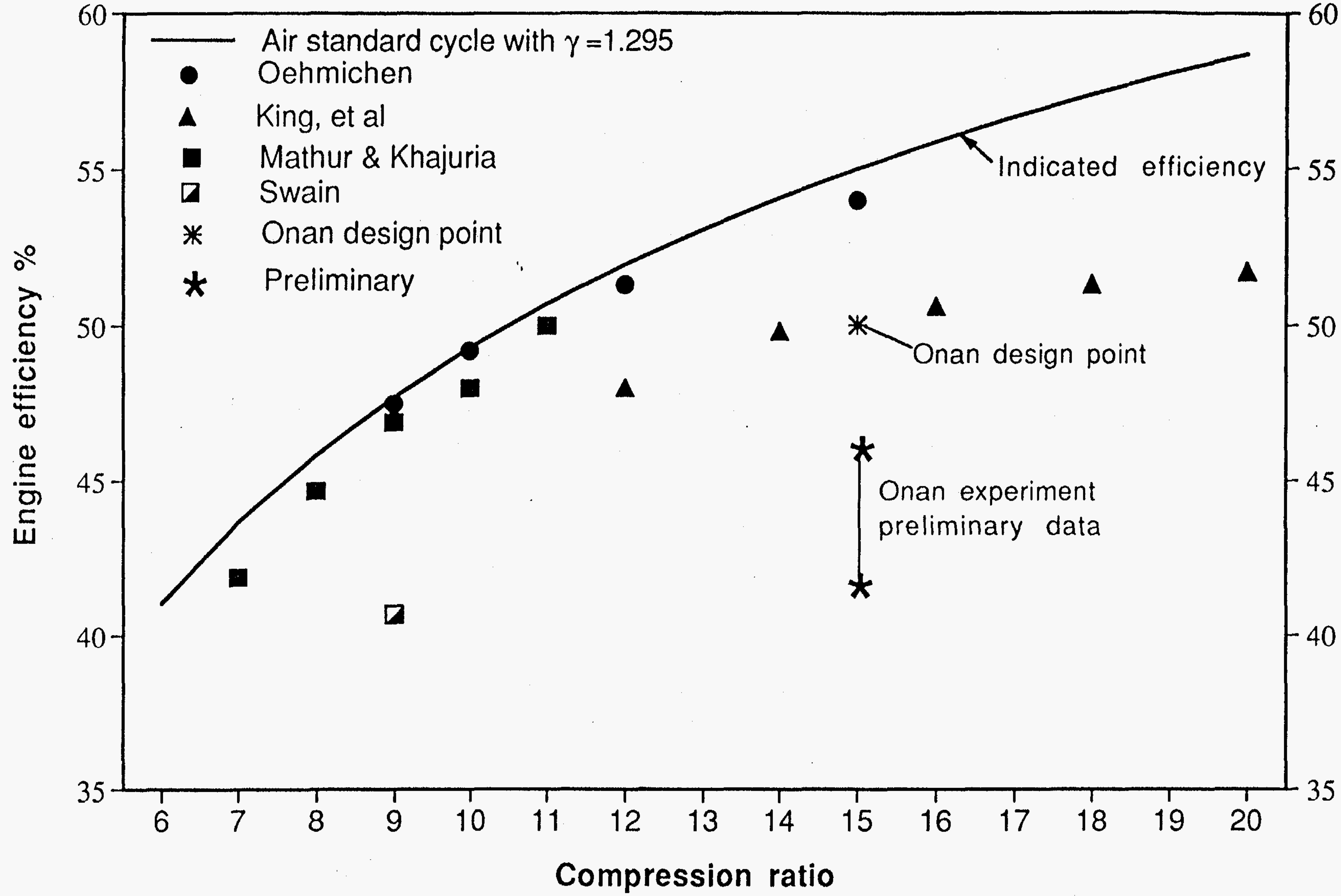
Air standard cycle with γ =1.295
Oehmichen
King, et al
Mathur & Khajuria
Swain
Onan design point
Preliminary
Indicated efficiency
Onan design point
Onan experiment
preliminary data
Engine efficiency %
Compression ratio
60
55
50
45
40
35
6
7
8
9
10
11
12
13
14
15
16
17
18
19
20

Figure 5

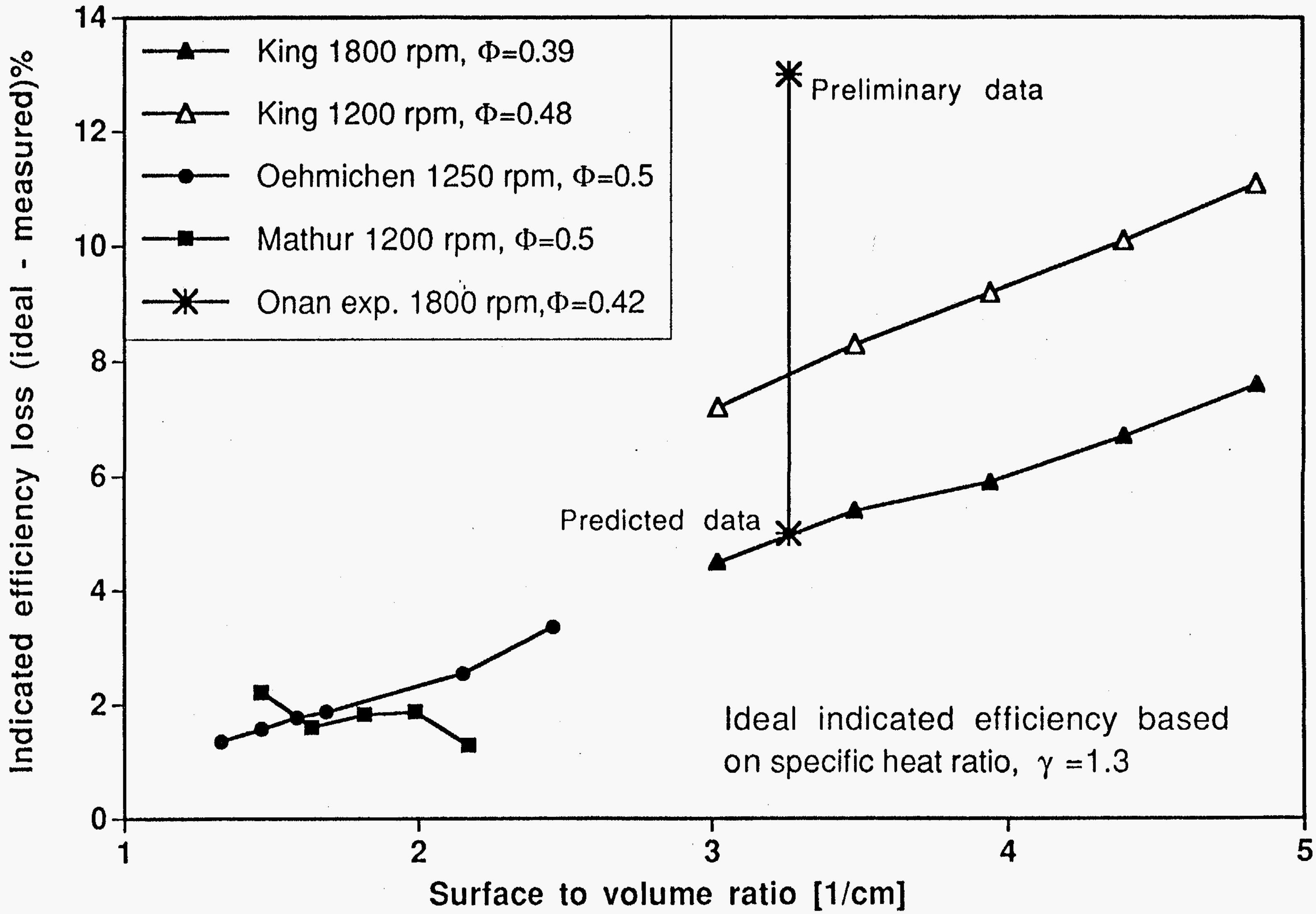
King 1800 rpm, Φ=0.39
King 1200 rpm, Φ=0.48
Oehmichen 1250 rpm, Φ=0.5
Mathur 1200 rpm, Φ=0.5
Onan exp. 1800 rpm,Φ=0.42
Preliminary data
Predicted data
Ideal indicated efficiency based on specific heat ratio, γ =1.3
Indicated efficiency loss (ideal - measured)%
Surface to volume ratio [1/cm]
0
2
4
6
8
10
12
14
1
2
3
4
5

Figure 6

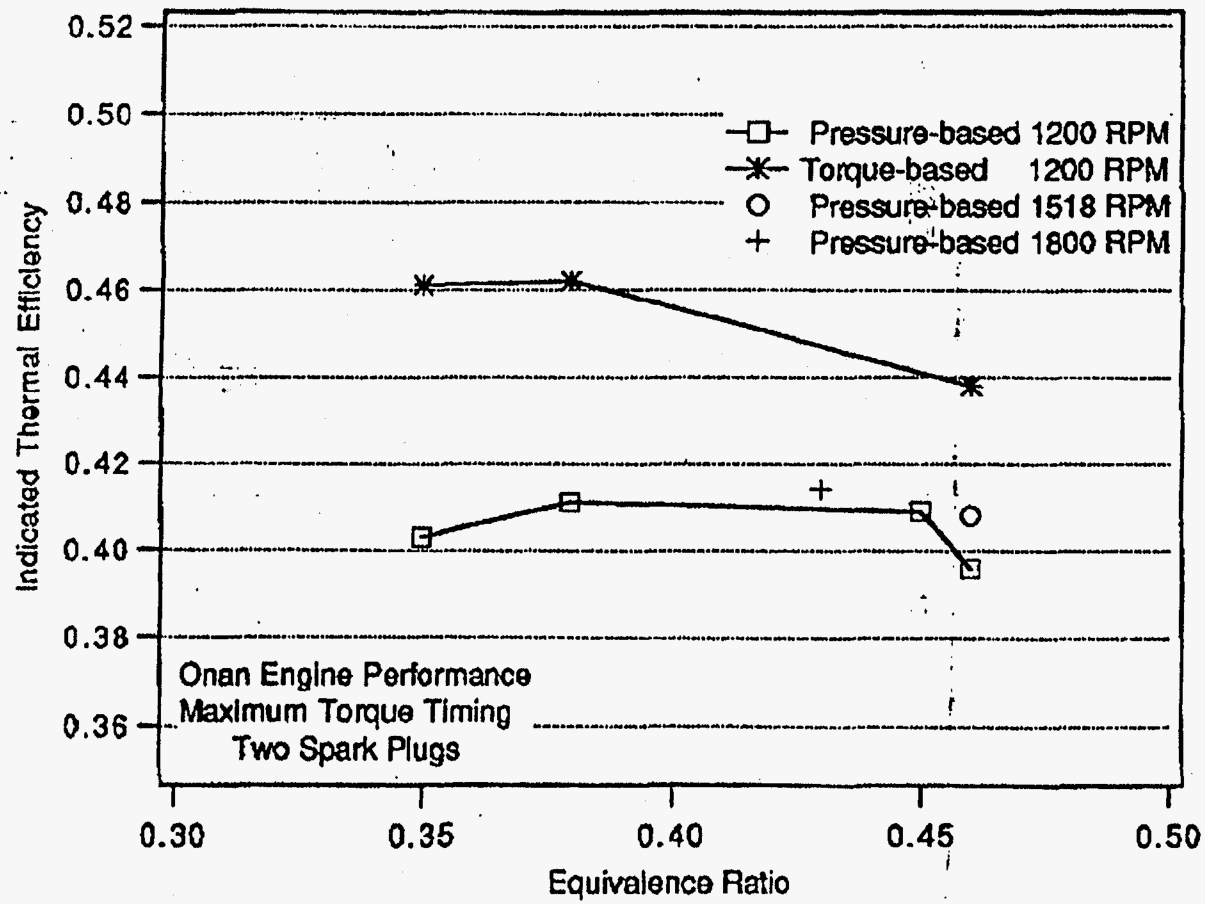

Figure ~~11~~. Onan indicated efficiency range

7